

Full Paper

A Scalable Route for the Regio- and Enantioselective Preparation of a Tetrazole Prodrug: Application to the Multi-Gram Scale Synthesis of a PCSK9 Inhibitor

Anne Akin, Mark T Barrila, Thomas A Brandt, Anne-Marie Dechert-Schmitt, Pascal Dube, David D Ford, Adam S. Kamlet, Chris Limberakis, Andrew Pearsall, David W. Piotrowski, Brian Quinn, Sarah Rothstein, Jerry Salan, Liuqing Wei, and Jun Xiao

Org. Process Res. Dev., **Just Accepted Manuscript** • DOI: 10.1021/acs.oprd.7b00304 • Publication Date (Web): 08 Nov 2017

Downloaded from <http://pubs.acs.org> on November 9, 2017

Just Accepted

“Just Accepted” manuscripts have been peer-reviewed and accepted for publication. They are posted online prior to technical editing, formatting for publication and author proofing. The American Chemical Society provides “Just Accepted” as a free service to the research community to expedite the dissemination of scientific material as soon as possible after acceptance. “Just Accepted” manuscripts appear in full in PDF format accompanied by an HTML abstract. “Just Accepted” manuscripts have been fully peer reviewed, but should not be considered the official version of record. They are accessible to all readers and citable by the Digital Object Identifier (DOI®). “Just Accepted” is an optional service offered to authors. Therefore, the “Just Accepted” Web site may not include all articles that will be published in the journal. After a manuscript is technically edited and formatted, it will be removed from the “Just Accepted” Web site and published as an ASAP article. Note that technical editing may introduce minor changes to the manuscript text and/or graphics which could affect content, and all legal disclaimers and ethical guidelines that apply to the journal pertain. ACS cannot be held responsible for errors or consequences arising from the use of information contained in these “Just Accepted” manuscripts.



1
2
3
4
5
6
7
8
9
10
11
12
13
14
15
16
17
18
19
20
21
22
23
24
25
26
27
28
29
30
31
32
33
34
35
36
37
38
39
40
41
42
43
44
45
46
47
48
49
50
51
52
53
54
55
56
57
58
59
60

A Scalable Route for the Regio- and Enantioselective Preparation of a Tetrazole Prodrug: Application to the Multi-Gram Scale Synthesis of a PCSK9 Inhibitor

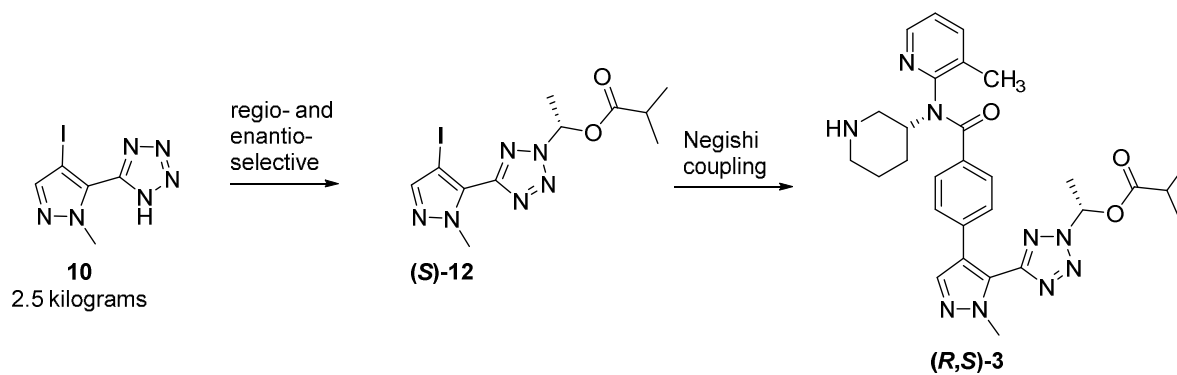
Anne Akin,[‡] Mark T. Barrila,[‡] Thomas Brandt,[‡] Anne-Marie R. Dechert-Schmitt,[†] Pascal Dube,[#] David D. Ford,[#] Adam S. Kamlet,[†] Chris Limberakis,[†] Andrew Pearsall,[#] David W. Piotrowski^{†}, Brian Quinn,[#] Sarah Rothstein,[#] Jerry Salan,^{*#} Liuqing Wei,[†] Jun Xiao[†]*

[†]Medicine Design, Pfizer, Inc., Eastern Point Road, Groton, Connecticut, 06340, United States

[‡]Chemical Research and Development, Pfizer, Inc., Eastern Point Road, Groton, Connecticut 06340, United States

[#]Nalas Engineering Services, Inc., 85 Westbrook Road, Centerbrook Connecticut 06409, United States

TOC/Abstract graphic



1
2
3 ABSTRACT: The synthesis of multi-gram quantities of a small molecule PCSK9 inhibitor (*R,S*)-**3** is
4 described. The route features a safe, multi-kilogram method to prepare 5-(4-iodo-1-methyl-1*H*-
5 pyrazol-5-yl)-2*H*-tetrazole (**10**). A three-component dynamic kinetic resolution (DKR) between
6 tetrazole **10**, acetaldehyde and isobutyric anhydride was catalyzed by a chiral DMAP catalyst to
7 afford enantiomerically enriched hemiaminal ester (*S*)-**12** on multi-kilogram scale. Magnesiumation,
8 transmetallation and Negishi coupling provided access to Boc-intermediate (*R,S*)-**13**, which was
9 deprotected to provide (*R,S*)-**3** in multi-gram quantities.
10
11
12
13
14
15
16
17
18
19

20
21 Keywords: PCSK9, tetrazole, DKR, cross-coupling
22
23

24 Introduction

25
26 High serum LDL-cholesterol (LDL-C) is a risk factor for atherosclerosis and a widely recognized
27 biomarker for increased risk of coronary heart disease (CHD). When pharmaceutical intervention is
28 required to lower LDL-C, statins (e.g. Lipitor[®], Crestor[®]) are often used as frontline treatment.
29 However, in some cases, these agents do not provide sufficient lowering of LDL-C. Inhibition of
30 proprotein convertase subtilisin/kexin type 9 (PCSK9) has emerged as a promising new target for
31 decreasing serum LDL-C levels and reducing risk of CHD. Of note, mAbs such as alirocumab and
32 evolocumab are approved injectable drugs.¹ Previous disclosures from the Pfizer laboratories
33 described small molecule inhibitors of PCSK9, PF-00932239 (**1**) and PF-06446846 (**2**).²
34 Subsequent optimization work led to the identification of tetrazole pro-drug (*R,S*)-**3**. The synthetic
35 challenges associated with the large scale synthesis of (*R,S*)-**3** include the hazards of preparing a
36 tetrazole, regio- and enantioselective formation of a tetrazole hemiaminal ester, and the subsequent
37
38
39
40
41
42
43
44
45
46
47
48
49
50
51
52
53
54
55
56
57
58
59
60

chemistry and handling of these base-sensitive species. Herein, we disclose a safe and scalable route directed toward multi-gram quantities of (*R,S*)-**3** to support preclinical toxicology studies.

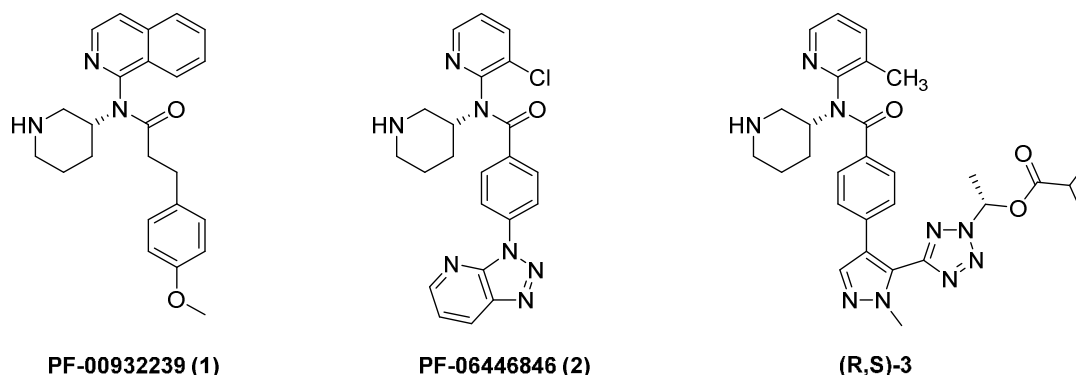
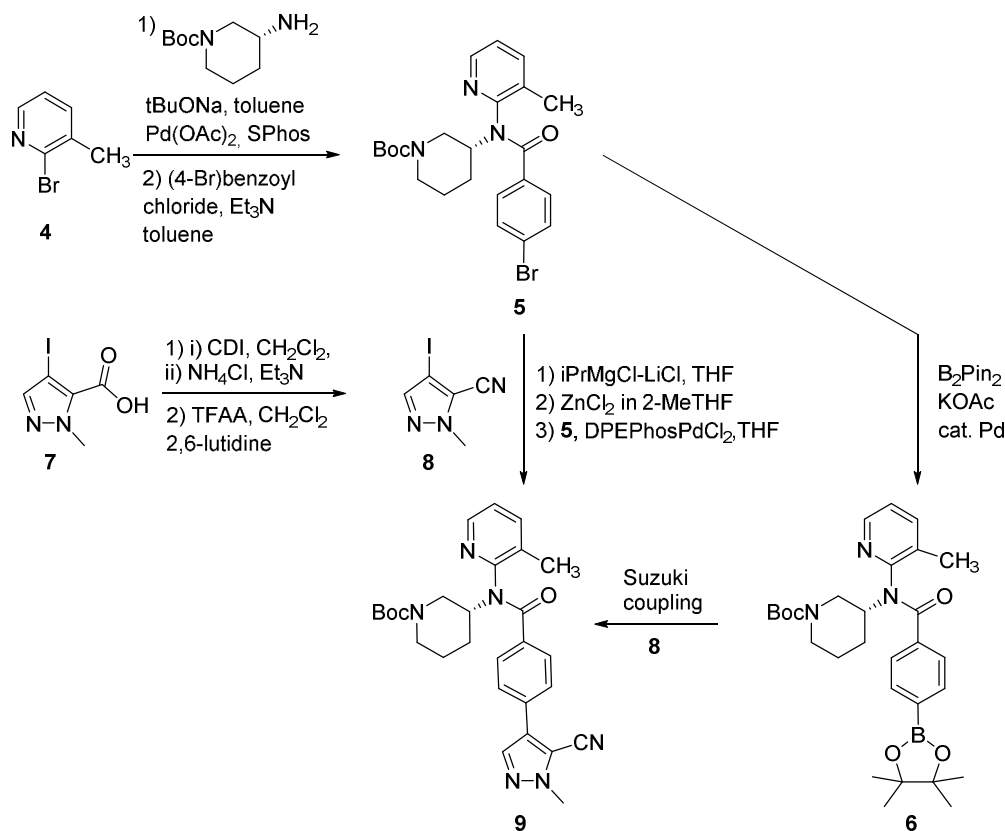


Figure 1. Small molecule PCSK9 inhibitors

Medicinal Chemistry Routes to **3**

Two versatile synthetic intermediates, tertiary amide **5** and iodopyrazole **8**, were critical for implementation of the early medicinal chemistry routes (Scheme 1). Amide **5** was synthesized in two steps via Buchwald amination followed by acylation with 4-bromobenzoyl chloride in the presence of base. Conversion of **5** into pinacol boronate **6** then offered a range of opportunities to append a distal heteroaryl group by Negishi (from **5**) or Suzuki-Miyaura (from **6**) cross-coupling methodologies (Scheme 1). Nitrile **8** was synthesized in three steps from the commercially available 4-iodo-3-methylpyrazole-5-carboxylic acid (**7**) by conversion to the acyl imidazole and ammonolysis followed by dehydration. The Negishi coupling of **5** with **8** provided cyanopyrazole **9** in 80% yield, but the Suzuki-Miyaura coupling of **6** with heteroaryl halides (e.g. coupling of pyrazole **8** to give **9**) was generally favored for analog synthesis.

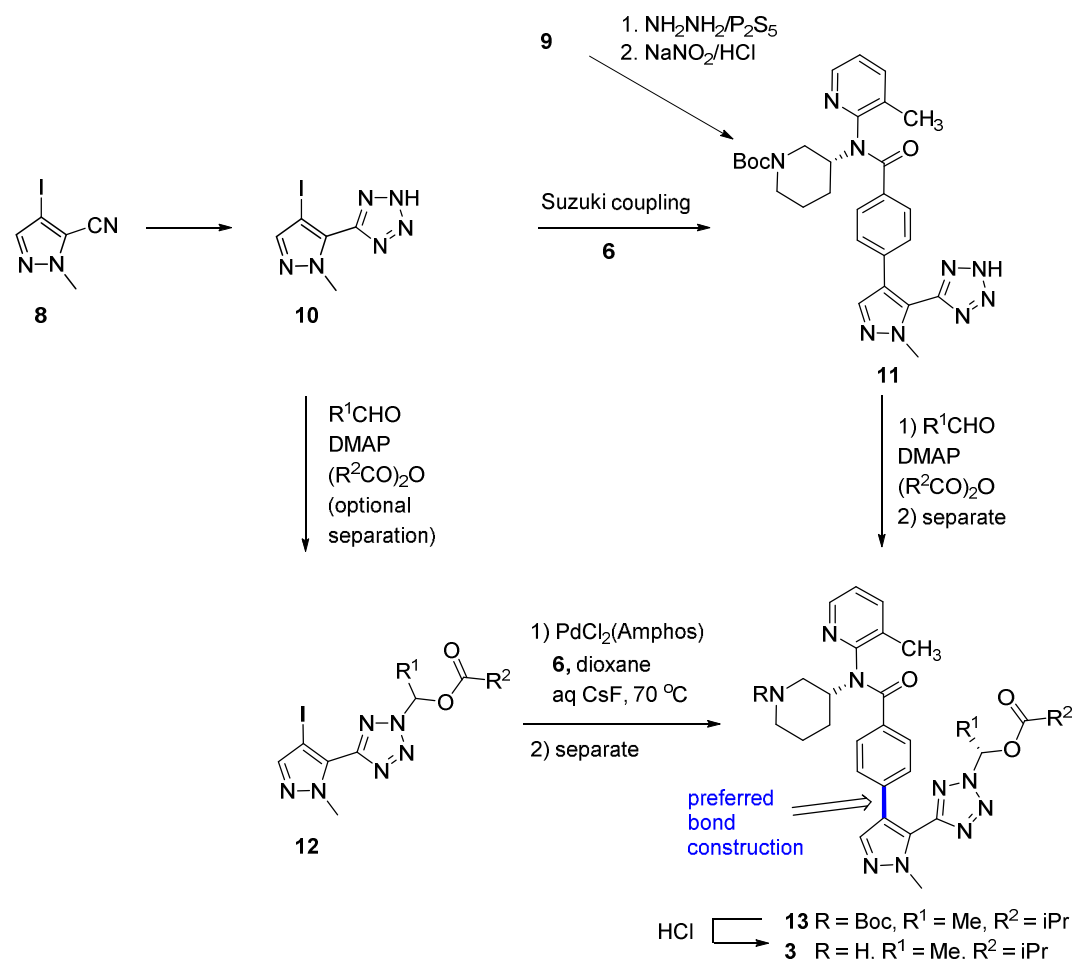
Scheme 1: Medicinal Chemistry Routes to Synthetic Intermediates



With due caution, installation of the tetrazole was investigated next. The conversion of nitriles into tetrazoles with hydrazoic acid is well known.³ Small scale preparation (ca. 0.5 g) of tetrazole **10** could be effected by reaction of **8** with hydrazoic acid, made in situ from NaN₃ and NH₄Cl, at high temperature. However, the toxic and shock-sensitive nature of hydrazoic acid based reagents led to exploration of alternative routes to tetrazoles. In brief, nitriles **8** or **9** could be converted into tetrazoles **10** or **11** by reaction of hydrazine with a thioamide to provide the amidrazone, formed in situ, and cyclized with nitrous acid. While this method avoided the use of hydrazoic acid, it employed the toxic hydrazine and the unstable nitrous acid. Further work toward tetrazoles via this route was abandoned. However, the availability of tetrazole **10** allowed for investigation of cross-

1
2
3 coupling reactions of it or a protected version thereof (e.g. compound **12**). The successful outcome
4
5 of the cross-coupling with either tetrazole substrate **10** or **12** was not clear since the presence of an
6
7 acidic hydrogen on **10** could interfere with typical coupling conditions or the base-labile hemiaminal
8
9 ester **12** could suffer premature hydrolysis under typical Suzuki-Miyaura reaction conditions. Prior
10
11 to the recent report from Buchwald,⁴ cross-coupling of aryl or heteroaryl halides containing acidic
12
13 hydrogens was viewed as difficult; a trace of desired coupled product **11** was obtained with these
14
15 reported conditions. After extensive investigation and high-throughput screening, an optimized set
16
17 of conditions (aq. NaOH, Pd(OAc)₂, cataCXium[®] A, dioxane 70-100 °C) allowed for facile coupling
18
19 of **10** with **6** on 1 g scale to provide tetrazole **11** in 92% isolated yield. Likewise, using racemic
20
21 hemiaminal substrate **12**,⁵ high-throughput screening led to identification of a set of mild, fluoride-
22
23 based Suzuki-Miyaura coupling conditions that provided a high yield of coupled product **13**. The
24
25 medicinal chemistry routes as described above were practical for analog generation when coupled
26
27 with chromatography on chiral support to separate either hemiaminal ester **12** or **13** (Scheme 2). The
28
29 late stage separation and N-Boc deprotection not only gave desired product (*R,S*)-**3**, but also
30
31 provided access to valuable diastereomeric standards (*R,R*)-**13**, (*R,S*)-**13**, and (*R,R*)-**3**. Furthermore,
32
33 the absolute stereochemistry of (*R,R*)-**3** was determined from the X-ray crystal structure.⁶ The
34
35 stereochemistry of the desired diastereomer (*R,S*)-**3**, could thus be inferred from this structure.
36
37
38
39
40
41
42
43
44
45
46
47
48
49
50
51
52
53
54

Scheme 2: Medicinal Chemistry Routes to Tetrazole Intermediates and Product 3



As (*R,S*)-**3** emerged as a potential candidate compound, our attention turned toward a safe, scalable route. Our preferred approach for the construction of **3** was to perform a cross-coupling between hemiaminal ester **12** and benzamide **5** or **6**. This option afforded the ability to independently investigate the large scale preparation of tetrazole **10**, a method to synthesize a single enantiomer of **12** and optimized coupling conditions for **13**. With these bond connections in mind, an efficient, scalable route to **3** was undertaken.

1
2
3 The original conditions used to prepare tetrazole **10** relied on the treatment of nitrile **8** with
4
5 hydrazoic acid generated in situ from NaN_3 and NH_4Cl in DMF at temperatures above 100 °C.
6
7 Although convenient for small scale preparation, the generation of anhydrous hydrazoic acid posed
8
9 serious safety concerns. Hydrazoic acid is highly toxic, and is a sensitive energetic compound in
10
11 concentrated solutions and vapors with a low detonation threshold.⁷ Additionally, it has a boiling
12
13 point of 37 °C, and it can potentially condense in cooler areas of the reactor, from mechanical parts
14
15 to ductwork. Condensed hydrazoic acid could then explode when the equipment is being
16
17 disassembled or cleaned. Moreover, the original conditions risk the formation of ammonium azide,
18
19 another powerful explosive, as a by-product.⁸ Furthermore, the target tetrazole **10** had the potential
20
21 to be an energetic compound itself, a concern that warranted further safety evaluation.
22
23
24

25
26 The medicinal chemistry route involved the treatment of nitrile **8** with an excess of NaN_3 and
27
28 NH_4Cl in DMF at 120 °C. After reaching completion (ca. 20 h), the excess azide was neutralized
29
30 with nitrous acid (prepared in situ from the stepwise addition of aq NaNO_2 and dilute H_2SO_4). This
31
32 operation, while very effective in consuming the residual azide, was found to be exothermic with
33
34 concurrent generation of nitrogen gas. Moreover, even on small scale, the quench resulted in the
35
36 formation of a solid mass that impeded stirring. This significant co-precipitation of inorganic salts,
37
38 potentially including ammonium azide, necessitated extensive washing of the solids obtained by
39
40 filtration before isolation of tetrazole **10** in ca. 85–90% yield.
41
42
43
44

45 Given the risk of explosion associated with producing hydrazoic acid at high levels during the
46
47 reaction, we reasoned that using water as a co-solvent could facilitate the reaction by increasing the
48
49 solubility of the inorganic salts while desensitizing the hydrazoic acid contained in the gas phase
50
51 towards a potential explosion.⁹ This hypothesis was confirmed when >99.5% conversion was
52
53
54

1
2
3 obtained in 16 h at 90 °C using DMF/water (2:1). Further dilution of the reaction mixture with
4
5 additional water followed by the standard neutralization protocol mitigated risks in the isolation
6
7 procedure while producing **10** as a crystalline white solid. This procedure allowed for reproducible
8
9 preparation of high purity material in 88–93% yield. Tetrazole **10** was found to be insensitive to
10
11 impact using the Bruceon method on a BAM Fallhammer, showing no sign of decomposition in six
12
13 trials at 100 cm with a 10 kg hammer weight. Moreover, a similar evaluation of its sensitivity
14
15 towards friction using a BAM friction instrument again showed no event even at 360 N, thus
16
17 confirming the stability of tetrazole **10** towards impact and friction.¹⁰
18
19

20
21 A recent report summarized the broad range of reaction conditions to synthesize tetrazoles from
22
23 nitriles.¹¹ In light of the reports of the use of Lewis acids, in particular zinc salts, to catalyze
24
25 tetrazole formation with reduced hydrazoic acid levels,¹² we evaluated these catalysts for the
26
27 conversion of nitrile **8** into tetrazole **10**. The use of zinc oxide in THF/water led to modest
28
29 conversion (<40%) after prolonged reaction times at reflux. A broader screen of catalysts revealed
30
31 that ca. 70% conversion could be obtained using 10 mol% zinc bromide in THF/water (1:2).
32
33 Interestingly, the reaction pH was measured to be of 7.5, suggesting that the equilibrium between
34
35 azide and hydrazoic acid ($\text{pK}_a = 4.6$)¹³ was shifted significantly toward azide, offering hope that
36
37 levels of hydrazoic acid could be managed to safe levels. The slow reaction rate led us to screen a
38
39 variety of organic co-solvents to identify an alternative to THF that would allow us access to higher
40
41 temperatures. We performed these reactions using 10 mL of water per gram of starting material, and
42
43 5 mL of the organic solvent per g of **10** (Table 1). Our study revealed that alternative organic co-
44
45 solvents provided a significant increase in conversion compared with the original THF solvent
46
47 system. Interestingly, the reactions with ethanol and ethylene glycol both showed significant
48
49
50
51
52
53
54

1
2
3 accumulation of nitrile **8** on the walls of the test tube used to run the reaction, presumably due to
4
5 sublimation. This makes those solvents less practical. We were pleased to find that DMF and IPA
6
7 both led to high conversion at this small scale with traces of **8** accumulated on the walls for DMF
8
9 and none detectable with IPA. We thus selected IPA as the co-solvent of choice for the system under
10
11 evaluation.
12
13

14 **Table 1.** Solvent Screen for the Formation of the Tetrazole **10** with ZnBr₂.^a
15
16

Entry	Organic co-solvent	Conversion after 24 h
1	MeTHF	45%
2	DMF	86%
3	EtOH	80%
4	IPA	89%
5	Ethylene glycol	90%

17
18
19
20
21
22
23
24
25
26
27
28
29 ^aReaction conditions: 100 mg nitrile **8** in 1 mL water, 0.5 mL organic solvent, 2 eq NaN₃ and 0.1 eq ZnBr₂ at 80 °C.
30
31
32

33 The next step was to evaluate the impact of concentration and solvent ratio on the reaction
34
35 outcome. A series of reactions was conducted using 20 mL of solvent/g in order to stress the
36
37 reaction conversion under high dilution (Table 2). Although the solvent range evaluated was broad,
38
39 the study showed that a 1:1 ratio of water to IPA seemed to provide a suitable environment for the
40
41 smooth formation of **10**. Additional control experiments showed that only trace amounts of **10** are
42
43 formed when the reaction is conducted in water or IPA alone. As full conversion was achieved after
44
45 48 h at 80 °C, these conditions routinely provided >80% yield of >98% potency of **10** after
46
47 treatment under the standard isolation procedure.
48
49
50
51

52 **Table 2.** Impact of Solvent Composition for the Formation of Tetrazole **10** catalyzed by ZnBr₂
53
54

Entry	Ratio Water-IPA	Conversion after 24 h (48 h)	Accumulation of nitrile 8 on walls?
1	1:3	77% (92%)	No
2	1:1	88% (97%)	No
3	3:1	61% (82%)	Yes

*Reaction conditions: 100 mg nitrile **8** in 2 mL of solvent (water + IPA), 2 eq NaN₃ and 0.1 eq ZnBr₂ at 80 °C.

With an improved solvent composition determined, we turned our attention back to the effect of the stoichiometry of NaN₃ and ZnBr₂ on conversion. We found that 2 equiv of NaN₃ were enough to obtain 98% conversion after 48 h at 80 °C. While lower quantities led to a more sluggish reaction, increased catalyst loading showed no further advantage from a conversion and purity standpoint. The subsequent evaluation of the impact of the ZnBr₂ stoichiometry revealed that a 10 mol% loading was necessary to achieve high conversion (98% after 48 h at 80 °C). Poor conversion was obtained when using 5 mol% ZnBr₂. It is noteworthy that using 20 mol% of catalyst was found to increase the rate of the reaction and provide 95% conversion in 16 h. As higher catalyst loadings may lead to a greater quantity of hydrazoic acid produced via hydrolysis of ZnBr₂ to form HBr, we opted to maintain a low stoichiometry of ZnBr₂ at the expense of reaction time. Thus, the optimal conditions on small scale featured 2 equiv NaN₃, 10 mol% ZnBr₂ in 5 volumes of water and 5 volumes of IPA at 80 °C to provide 98% conversion in 48 h while maintaining the reaction mixture above pH 7.

Upon optimization of the stoichiometry, the selected process was evaluated to determine the levels of hydrazoic acid present in the reactor headspace. This was achieved using gas-phase FTIR to monitor gases leaving the reactor vent while a constant gas sweep was applied to the reactor. Off-line ion chromatography was also used to provide complementary data for this study by analyzing a scrubber downstream of the IR cell. The original conditions (NaN₃, NH₄Cl, DMF, 120 °C) were also

1
2
3 evaluated for comparison. To test if the removal of hydrazoic acid in the gas sweep was negatively
4
5 impacting the reaction, we executed a control experiment by performing a small scale reaction using
6
7 the ZnBr₂ conditions subjected to a constant air sweep. A 200 mg reaction was thus performed in an
8
9 EasyMax™ reaction tube with magnetic stirring equipped with an air sweep vented into two water
10
11 scrubbers in series to capture any hydrazoic acid that would escape. This safety measure was found
12
13 to only have minimal impact on the chemistry, with 86% conversion achieved after 24 h at 80°C and
14
15 92% after 40 h. Excess azide was destroyed by sequential addition of aq NaNO₂ and H₂SO₄, and
16
17 tetrazole **10** was obtained in 80% yield after filtration and drying. Analyzing the water scrubber by
18
19 ion chromatography revealed the presence of less than 200 ppm (w/v) of hydrazoic acid in the first
20
21 10 mL scrubber (i.e. 2 mg hydrazoic acid trapped), supporting the assertion that only traces of
22
23 hydrazoic acid had formed during the reaction and its removal does not negatively impact the
24
25 chemistry. The absence of hydrazoic in the second water trap confirms that the hydrazoic acid
26
27 evolved was effectively trapped in the first water scrubber.
28
29
30
31
32

33 Control experiments with ZnBr₂ in the absence of nitrile **8** were conducted to quantify the
34
35 maximum possible levels of hydrazoic acid under these conditions. A reaction was performed
36
37 following the material balance (Table 3). It is noteworthy that the reaction was performed using the
38
39 same reaction volume, solvent, and head space available as in the calibration experiments to ensure
40
41 the direct correlation of the data. The reagents were thus mixed at ambient temperature and heated to
42
43 80 °C while under monitoring by gas-phase FTIR. The FTIR profile of this reaction showed that no
44
45 detectable level of hydrazoic acid is present in the head space prior to heating the mixture (Figure 2).
46
47 Upon equilibration at 80 °C, the system reached a steady state where the absorption was constant
48
49 over time at approximately 400–500 ppm. Cooling the reaction mixture back to 20 °C led to the
50
51
52
53
54

disappearance of the hydrazoic acid peak by FTIR. The reactor was swept with N₂ at a gas flow rate of 0.79 mL/s, so at the average concentration of 410 ppm, this corresponds to a mass flow rate of 2.1 mg/h of hydrazoic acid. The area under the curve was calculated to be 189.4 AU s, corresponding to a total of 3.1 mg of hydrazoic acid produced during the course of this experiment. At the end of the experiment, a sample of the scrubber solution was analyzed by ion chromatography, revealing a 136 ppm concentration of azide (w/v as hydrazoic acid), representing 1.4 mg of hydrazoic acid dissolved in the 10 mL scrubber. This number suggests that the scrubber was only partially adept at capturing the hydrazoic acid formed, or that some hydrazoic acid was adsorbed in the tubing leading to the scrubber.

Table 3. Material Balance for the Evaluation of ZnBr₂ Catalyst in the Absence of Nitrile

Reagent	Quantity	mmol (ratio)
NaN ₃	1.73 g	26.66 (20)
Water	15.0 mL	
IPA	15.0 mL	
ZnBr ₂	0.30 g	1.33 (1)
HN ₃	1.15 g ^a	26.66

^aexpected maximum amount of hydrazoic acid

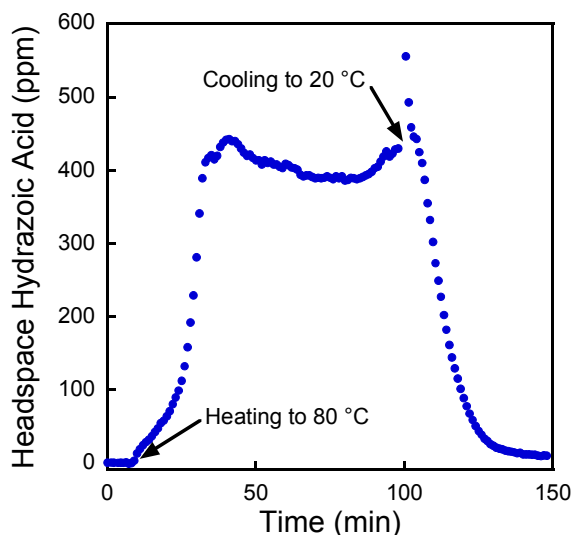


Figure 2. Headspace hydrazoic acid levels measured by gas phase FTIR under ZnBr_2 conditions.

The advantages and disadvantages of the three different processes are compared to highlight the differences between them (Table 4). The original conditions offered a slow release of hydrazoic acid due to its heterogeneous nature but the isolation conditions were not suitable for scale-up. Either of the modified conditions, generation 1 or 2, was suitable for scale up. Generation 1 provided a higher yield and a higher throughput. However, the homogeneity of the reaction led to the highest levels of hydrazoic acid measured, which could be mitigated by an appropriate sweep of the reaction headspace to a scrubber to ensure the neutralization of hydrazoic acid. Alternatively, the second generation conditions offered the lowest levels of hydrazoic acid at the expense of reaction rate and throughput. With either of these last two processes, tetrazole **10** was isolated in >99% potency through the improved isolation protocol.

Table 4: Comparison of Methods to Convert Nitrile **8** into Tetrazole **10**

Process	Yield	Throughput	HN_3 in	Pros	Cons
---------	-------	------------	------------------	------	------

headspace					
Original 2.4 equiv NaN ₃ , 3.0 equiv NH ₄ Cl, DMF, 120 °C	85%	90 g/L ^a	> 3800 ppm	•Heterogeneous; slow release of HN ₃	•High HN ₃ levels •Heterogeneous; potential mass transfer issues
Generation 1 2 equiv NaN ₃ , 2 equiv NH ₄ Cl, DMF/water, 90 °C	85-90%	80 g/L	8000 ppm	•Homogeneous •HN ₃ hazards mitigated by water scrubber	•High HN ₃ levels
Generation 2 2 equiv NaN ₃ , 0.1 equiv ZnBr ₂ , IPA/water, 75-80 °C	80%	< 40 g/L	410 ppm	•Low HN ₃ levels	•Longer reaction time (48 h) •Potential for reaction to stall (catalyst deactivation) •Lower yield

^aForms a solid mass preventing stirring. Majority of precipitate washed away on filter through extensive washing. Volume not included in calculation.

With a safe, scalable method to synthesize tetrazole **10**, we turned our attention to improvement of the final steps in the sequence. Our previously reported conditions for the regio- and enantioselective synthesis of tetrazole hemiaminal esters⁵ demonstrated that the more sterically accessible nitrogen of the tetrazole (N-2) reacts with aldehydes at a faster rate to provide the hemiaminal intermediate. In the presence of a (chiral) DMAP catalyst, the tetrazole-2-hemiaminal is preferentially acylated while the tetrazole-1-heminal can be acylated (slower) or revert back to aldehyde and tetrazole starting materials. The conditions were optimized for the scaled synthesis of **12** by examination of solvent, concentration, equivalents of acetaldehyde, and catalyst loading. Reactions employed 2 equiv of acetaldehyde, 1.5 equiv of isobutyric anhydride, and 1.5 equiv of Et₃N per equivalent of tetrazole **10**. MTBE was used in place of diethyl ether as it is less prone to form hazardous peroxides and favored for process scale reactions. Next, it was determined that in order to drive the reaction to completion, 3 mol% of Connon's catalyst **14** was required (overnight reaction time). The use of 1 mol% of catalyst led to reaction stalling and approximately 15% of the

starting material tetrazole unconsumed. To optimize the enantioselectivity on large scale, the reaction was executed at various temperatures. Holding the reaction temperature at 0 °C led to improved enantioselectivity compared to ambient temperature (92 vs 83% *ee*), though lowering the temperature to -20 °C provided a marginal improvement (93% *ee*). Finally, various dilution conditions ranging from 20 mL/g to 75 mL/g were tested for effects on enantioselectivity (see Table 5, results at 0 °C). With higher dilution, tetrazole hemiaminal ester **12** was formed in higher enantiomeric ratio. Ultimately, 50 mL/g and 0 °C were chosen for scale-up conditions due to tank capacity and convenience. On a 2.5 kg scale, tetrazole **10** was converted into **12** in a regioselective and enantioselective manner using catalyst **14** (189 g, 3 mol%). The prodrug fragment **12** was obtained in quantitative yield and an enantiomeric ratio (97:3) before removal of the minor enantiomer by chiral preparative chromatography.

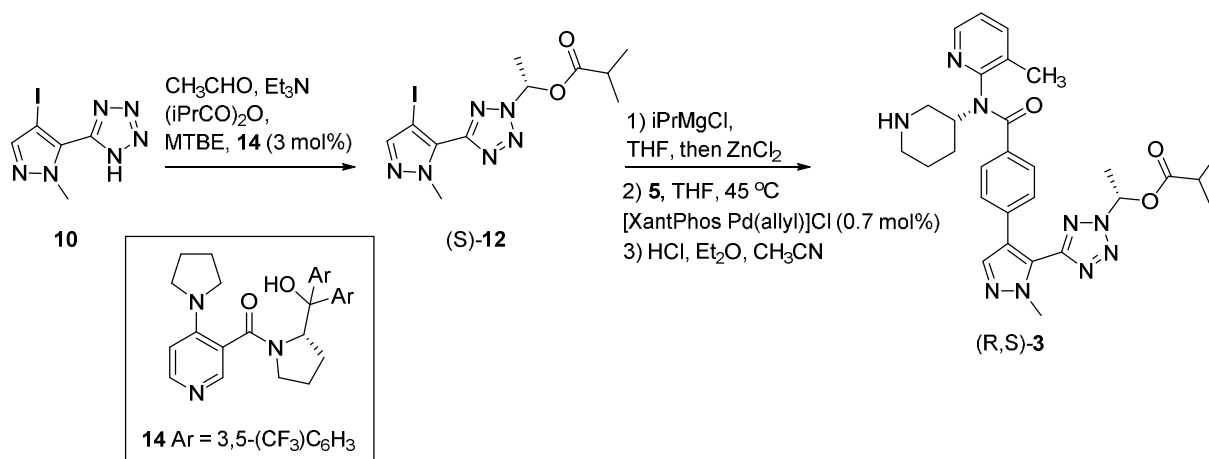
Table 5. Small Scale Assessment of Dilution/Enantioselectivity Correlation for Tetrazole **12**

Dilution (mL MTBE/g 10)	concentration	% <i>ee</i> 12
20	0.18 M	87
25	0.14 M	90
36	0.10 M	91
50	0.07 M	92
75	0.05 M	94

With a reliable route to **12** in hand, the merits of the previously examined cross-coupling methods were assessed. The Suzuki coupling was favored for routine analog synthesis primarily for reasons of small-scale reliability and convenience. However, in the interest of minimizing step-count and avoiding the introduction of a potentially genotoxic boronic acid or ester,¹⁴ the appeal of the Negishi

coupling came to the fore for large scale reactions. In the event, magnesiation of tetrazole (*S*)-**12** was conducted by treatment with 1.3 equiv *i*PrMgCl at -45 °C. After 10 min, transmetalation to the organozinc was accomplished by addition of a 1.9 M solution of ZnCl₂ in 2-MeTHF (-45–23 °C, 1 h). Addition of bromide **5** and Pd-catalyst effected a rapid Negishi coupling (45 °C, 10 min, > 96% conversion). In order to ensure high purity of the base labile (*R,S*)-**3**, minor impurities from the Negishi coupling step were removed by chromatography to provide (*R,S*)-**13**. The intermediate **13** was deprotected with HCl to provide 241 g (89%) of (*R,S*)-**3** as a partially crystalline solid suitable for use in in vivo studies (Scheme 3).

Scheme 3. Hemiaminal Ester Synthesis and Negishi Coupling



Conclusions and Summary

Scalable methods to synthesize multi-kilogram quantities of 5-(4-iodo-1-methyl-1*H*-pyrazol-5-yl)-2*H*-tetrazole (**10**) were evaluated. A thorough safety assessment was conducted to ensure proper handling of hydrazoic acid/ammonium azide and tetrazole **10**, which allowed for identification of a few scalable methods. A three-component DKR between tetrazole **10**, acetaldehyde and isobutyric anhydride was catalyzed by a chiral DMAP catalyst to afford enantiomerically enriched hemiaminal

1
2
3 ester (*S*)-**12**. However, chromatography on chiral support was required to purge the undesired
4
5 enantiomer from this oil. Further optimization of the acylation would be required to avoid
6
7 chromatography. The end-game was enabled by a convergent Negishi coupling of hemiaminal ester
8
9 (*S*)-**12** with 4-bromobenzamide **5**. Further optimization of the Negishi coupling would be required to
10
11 avoid the late stage chromatography. Uneventful N-Boc deprotection with HCl in Et₂O provided
12
13 >240 g of (*R,S*)-**3**. Replacement of the ethereal solution of HCl for the N-Boc deprotection would be
14
15 an improvement to the process.
16
17
18
19
20

21 **Experimental Section**

22
23 All chemicals, reagents, and solvents were purchased from commercial sources when available and
24
25 used without further purification. Small scale reactions were magnetically stirred, and monitored by
26
27 thin layer chromatography (TLC) using pre-coated Whatman 250 μm silica gel plates and visualized
28
29 by fluorescence quenching under UV light. Air- and moisture-sensitive reactions were carried out
30
31 as described. Silica gel chromatography was performed using an ISCO system using ISCO pre-
32
33 packaged columns. Concentration under reduced pressure (in vacuo) was performed by rotary
34
35 evaporation at appropriate temperature and pressure. Purified compounds were further dried under
36
37 high vacuum to remove residual solvent. Yields refer to purified compounds. NMR spectra were
38
39 recorded with a Bruker spectrometer using a 5 mm BBFO probe at 400 MHz and 101 MHz for ¹H
40
41 and ¹³C acquisitions unless otherwise noted. Chemical shifts were referenced to the residual ¹H
42
43 solvent signals (CDCl₃, δ 7.27) and solvent ¹³C signals (CDCl₃, δ 77.16). Signals are listed as
44
45 follows: chemical shift in ppm (multiplicity identified as s = singlet, d = doublet, t = triplet, q =
46
47 quartet, m = multiplet, br = broad; coupling constants in Hz; integration). ELS detection was
48
49
50
51
52
53
54

1
2
3 performed using a Polymer Labs (Varian) 2100 ELS detector. Purities are reported as ELSD area
4
5 percent. High resolution mass spectroscopy (HRMS) was performed on a LC-MS TOF using a C18
6
7 2.5 μm 3.0 X 5.0 mm column at 60 $^{\circ}\text{C}$; ammonium formate: water as mobile phase A and 50:50
8
9 MeOH:MeCN as mobile phase B. Infrared spectra (FT-IR) were collected as neat liquid or solids on
10
11 ZnSe surface.
12
13

14
15
16
17 The level of hydrazoic acid in aqueous streams was measured using ion chromatography. It is
18
19 noteworthy that a water scrubber had to be used since aqueous hydroxide ions interfered with the
20
21 quantification of azide ions. A calibration curve was built using sodium azide solutions.
22
23

24 Ion Chromatography Method: Waters Ion-Pak anion HC (4.6 mm x 150 mm, Column T = 30 $^{\circ}\text{C}$);
25
26 Mobile Phase: 12/2/86 acetonitrile/butanol/borate–gluconate buffer; Flow rate: 2 mL/min; Injection:
27
28 50 μL ; Detection: Conductivity; Calibration: Sodium azide standard curve ($\sim 17\mu\text{g/mL}$ – 170 $\mu\text{g/mL}$
29
30 as hydrazoic acid).
31
32
33
34
35

36 Analytical UPLC-MS Method 1: Waters Acquity HSS T3 column (C_{18} 2.1 x 5 0 mm, 1.7 μ ; Column
37
38 T = 60 $^{\circ}\text{C}$); Gradient initial conditions: A-95%:B-5%; hold at initial from 0.0–0.1 min; linear Ramp
39
40 to A-5%:B-95% over 0.1–1.0 min; hold at A-5%:B-95% from 1.0–1.1 min; return to initial
41
42 conditions 1.1–1.5 min; mobile phase A: 0.1% formic acid in water (v/v); mobile phase B: 0.1%
43
44 formic acid in MeCN (v/v); flow rate: 1.25 mL/min.
45
46
47
48
49

50 Analytical UPLC-MS Method 2: Waters Acquity HSS T3 column (C_{18} 2.1 x 5 0 mm, 1.7 μ ,
51
52 Column T = 60 $^{\circ}\text{C}$); Gradient initial conditions: A-95%:B-5%; hold at initial from 0.00–0.10 min;
53
54

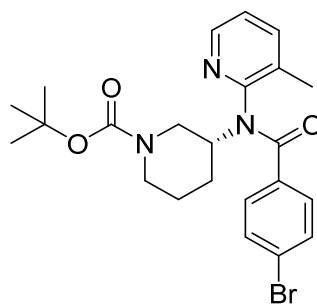
1
2
3 linear Ramp to A-5%:B-95% over 0.10–2.60 min; hold at A-5%:B-95% from 2.60–2.95 min; return
4
5 to initial conditions 2.95–3.00 min; mobile phase A: 0.1% formic acid in water (v/v); mobile phase
6
7 B: 0.1% formic acid in MeCN (v/v); flow rate: 1.25 mL/min.
8
9

10
11
12 Chiral Preparative Chromatography Method 1: Lux Amylose-2 column (500 mm x 21.2 mm, 5 μ ,
13
14 ambient temperature); mobile phase: 95% CO₂/5% 1:1 MeOH/MeCN; isocratic conditions; flow
15
16 rate: 80.0 mL/min.
17
18

19
20
21 Chiral Preparative Chromatography Method 2: Lux Amylose-2 column (250 mm x 50.0 mm, 5 μ ,
22
23 ambient temperature); mobile phase: 65% CO₂/35% MeOH; isocratic conditions; flow rate: 250
24
25 mL/min.
26
27

28
29
30
31 Analytical UPLC Method: BEH C₈ column (2.1 x 100 mm, 1.7 μ); mobile phase A: 50 mM
32
33 NaClO₄/0.1% H₃PO₄; mobile phase B: MeCN; UV detection at 210 nm; flow rate 0.5 mL/min;
34
35 gradient: initial conditions: A-95%:B-5%; linear ramp from 0.25–6.25 min; hold from 6.25–6.75
36
37 min; return to initial conditions 6.85–9.50 min.
38
39

40
41
42 *tert*-butyl (3*R*)-3-[(4-bromobenzoyl)(3-methylpyridin-2-yl)amino]piperidine-1-carboxylate (**5**)
43
44
45
46
47
48
49
50
51
52
53
54

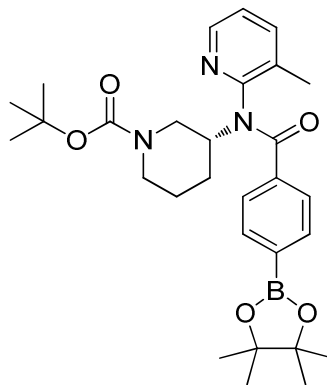


1
2
3
4
5
6
7
8
9
10
11
12
13
14 Step 1: A 500 L reactor was charged with 70.6 kg (10 volumes) of toluene, SPhos (320.0 g, 780
15 mmol, 0.02 equiv) and Pd(OAc)₂ (87.0 g, 360 mmol, 0.01 equiv) and the air in the headspace was
16 exchanged with N₂ (3x). After 2 h, 2-bromo-3-methylpyridine (8.0 kg, 46.8 mol, 1.25 equiv), *tert*-
17 butyl (3*R*)-3-aminopiperidine-1-carboxylate (7.5 kg, 37.5 mol, 1.00 equiv) and *t*BuONa (5.5 kg,
18 57.8 mol, 1.50 equiv) were added under N₂ atmosphere. The mixture was stirred at 80–90 °C for 5 h,
19 then cooled to 45 °C. The mixture was filtered through diatomaceous earth (3.9 kg). The pad was
20 rinsed with toluene (20 kg). The organic layer was washed with brine (2x 72 kg), concentrated to 10
21 volumes, treated with decolorizing carbon, filtered (2x diatomaceous earth), and concentrated to 3–4
22 volumes. The toluene was exchanged with heptane and the mixture was cooled to 0 °C. The solids
23 were filtered, the cake was washed with heptane and dried to give *tert*-butyl (3*R*)-3-[(3-
24 methylpyridin-2-yl)amino]piperidine-1-carboxylate 6.25 kg, (49%) with 96% area purity, 98.9%
25 assay. ¹H NMR (CDCl₃) δ 8.00 (d, 1H), 7.20 (d, 1H), 6.51(dd, 1H), 4.36 (br s, 1H), 4.16 (br s, 1H),
26 3.63 (d, 1H), 3.52 (br s, 2H), 3.36-3.30 (m, 1H), 2.06 (s, 3H), 1.90 (br s, 1H), 1.73 (br s 2H), 1.59
27 (br s, 1H), 1.38 (br s, 9H). ¹³C NMR (CDCl₃) δ 156.0, 155.3, 145.5, 136.8, 116.5, 112.7, 79.5, 49.0,
28 46.3, 43.8, 29.9, 28.4, 22.5, 17.0. HRMS (*m/z*) [M+Na]⁺ calcd for C₁₆H₂₅N₃NaO₂, 314.1839; found,
29 314.1833.
30
31
32
33
34
35
36
37
38
39
40
41
42
43
44
45
46
47
48
49
50
51
52
53
54
55
56
57
58
59
60

1
2
3 Step 2: A 500 L reactor was charged with toluene (78 kg, 14 volumes), DMF (250 g, 0.15 equiv)
4
5 and 4-bromobenzoic acid (5.2 kg, 25.7 mol, 1.2 equiv). The conduit was rinsed with toluene (5 kg).
6
7 The mixture was cooled to 10–20 °C, the reactor was charged with oxalyl chloride (4.2 kg, 33.1 mol,
8
9 1.6 equiv) and the head tank was rinsed with toluene. The mixture was warmed to 35 °C. After 4 h,
10
11 the mixture was concentrated to 5 volumes (residual oxalyl chloride < 0.05%). The tank was then
12
13 charged with toluene (48 kg), Et₃N (2.9 kg, 28.9 mol, 1.4 equiv) and *tert*-butyl (3*R*)-3-[(3-
14
15 methylpyridin-2-yl)amino]piperidine-1-carboxylate (6.2 kg, 21.3 mol, 1.0 equiv). The mixture was
16
17 stirred for 1 h at 10–20 °C, then heated at 80–90 °C. After about 10 h, the reaction was cooled to 10
18
19 °C and filtered. The cake was washed with toluene (10 kg). The filtrates were washed 2x 10 % citric
20
21 acid solution (65 kg) and 1x 1N NaOH (65 kg). The aqueous NaOH layer was extracted 1x toluene
22
23 (54 kg). The combined organic layers were concentrated to 7 volumes, then solvent exchanged with
24
25 heptane and cooled to 0–10 °C. After 5–10 h, the solids were isolated by centrifugation and dried for
26
27 16 h at 45 °C. Assay showed > 0.5% impurity. The solids were dissolved in toluene (42.5 L), washed
28
29 with 10% NaOH (2 h, 40–45 °C) and water (8.5 L). The organic layer was concentrated to 3–4
30
31 volumes. Heptane (4x 10 L) was added and the mixture concentrated at < 60 °C. After cooling to
32
33 20–30 °C, the solids were filtered, the cake was washed 1x heptane (4 L) and dried at 40–45 °C to
34
35 afford *tert*-butyl (3*R*)-3-[(4-bromobenzoyl)(3-methylpyridin-2-yl)amino]piperidine-1-carboxylate **5**
36
37 as a solid (7.0 kg, 77 %) with 99.3% HPLC area purity, 101.1 % assay. ¹H NMR (CDCl₃) δ 8.41 (br
38
39 s, 1H), 7.34 (br s, 1H), 7.25 (d, 2H), 7.16-7.14 (m, 3H), 4.65 (br s, 1H), 4.48 (br d, 1H), 4.15-4.04
40
41 (br m, 2H), 3.39 (br s, 1H), 2.55 (br s, 1H), 2.37 (br s, 1H), 2.01-1.98 (br d, 3H), 1.74 (br s, 1H),
42
43 1.47-1.43 (br d, 10H). ¹³C NMR (CDCl₃, 50 °C) δ 168.9, 154.8, 153.2, 146.8, 140.1, 135.6, 131.7,
44
45
46
47
48
49
50
51
52
53
54
55
56
57
58
59
60

1
2
3 130.8, 130.0, 124.4, 123.4, 79.6, 54.9, 48.0, 43.7, 28.4, 27.5, 25.1, 17.8. HRMS (m/z) $[M+Na]^+$
4
5 calcd for $C_{23}H_{28}BrN_3NaO_3$, 498.1189; found, 498.1190.
6
7
8

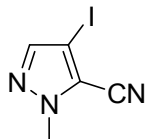
9
10 *tert*-butyl (3*R*)-3-[(3-methylpyridin-2-yl)[4-(4,4,5,5-tetramethyl-1,3,2-dioxaborolan-2-
11
12 yl)benzoyl]amino]piperidine-1-carboxylate (**6**)
13
14



28 A round-bottom flask was charged with *tert*-butyl (3*R*)-3-[(4-bromobenzoyl)(3-methylpyridin-2-
29
30 yl)amino]piperidine-1-carboxylate **5** (150 g, 317 mmol), bis(pinacolato)diboron (97.8 g, 381 mmol),
31
32 potassium acetate (100 g, 1.01 mol), and 2-MeTHF (750 mL). The reaction mixture was warmed to
33
34 75 °C. Pd(dppf)Cl₂·CH₂Cl₂ (5.12 g, 6.21 mmol) was added and the reaction mixture was heated
35
36 under reflux for 19 h. The reaction mixture was cooled to rt and water was added. The reaction
37
38 mixture was passed through a pad of diatomaceous earth and the layers were separated. The organic
39
40 layer was concentrated in vacuo. The brown residue was purified by column chromatography on
41
42 silica gel, eluting with a gradient of 30–50% EtOAc in heptane. The product-containing fractions
43
44 were concentrated in vacuo. The residue was filtered through a pad of diatomaceous earth using
45
46 warm heptane and DCM to solubilize product. The reaction mixture was concentrated in vacuo until
47
48 product started to crystallize. The solids were granulated for 16 h at rt, collected *via* filtration and
49
50
51
52
53
54

dried in a vacuum oven to afford *tert*-butyl (3*R*)-3-{(3-methylpyridin-2-yl)[4-(4,4,5,5-tetramethyl-1,3,2-dioxaborolan-2-yl)benzoyl]amino}piperidine-1-carboxylate **6** as a light pink solid (142 g, 86%). ¹H NMR (CDCl₃) δ 8.40 (m, 1H), 7.53-7.27 (m, 5H), 7.14-6.92 (m, 1H), 4.75-4.45 (m, 2H), 4.20-3.90 (m, 1H), 3.63-3.21 (m, 1H), 2.84-2.10 (m, 3H), 2.06-1.88 (m, 3H), 1.81-1.56 (m, 2H), 1.53-1.37 (m, 9H), 1.31 (s, 12H). ¹³C NMR (CDCl₃, 50 °C) δ 169.9, 154.8, 153.2, 146.6, 139.9, 139.1, 133.8, 131.9, 130.6, 127.5, 123.2, 83.9, 79.6, 54.7, 48.0, 43.7, 28.4, 27.6, 25.1, 24.8, 17.8. UPLC (UPLC-MS Method 1): t_R = 1.08 min. MS (ES⁺): 522.4 (M+H)⁺. HRMS (*m/z*) [M+H]⁺ calcd for C₂₉H₄₁BN₃O₅, 522.3139; found, 522.3144.

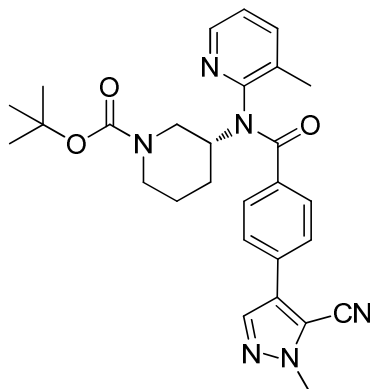
4-iodo-1-methyl-1*H*-pyrazole-5-carbonitrile (**8**)



Step 1: A round-bottom flask was charged with 4-iodo-1-methyl-1*H*-pyrazole-5-carboxylic acid (297 g, 1.18 mol), DCM (2.97 L), and 1,1'-carbonyldiimidazole (CDI) (207 g, 97% by mass, 1.24 mol). The reaction mixture was stirred at rt for 45 min. NH₄Cl (189 g, 3.53 mol) and Et₃N (498 mL, 3.53 mol) were added and the reaction mixture was stirred at rt overnight. The reaction mixture was concentrated in vacuo and the residue was suspended in water (~3 L) and granulated at rt for 1 h. The solid was collected via filtration, washed with water, and dried in a vacuum oven to afford 4-iodo-1-methyl-1*H*-pyrazole-5-carboxamide as a colorless solid (222 g, 75% yield). ¹H NMR (CDCl₃) δ: 7.53 (s, 1H), 6.56 (br s, 1H), 6.01 (br s, 1H), 4.21 (s, 3H). UPLC (UPLC-MS Method 1): t_R = 0.15 min. MS (ES⁺): 251.1 (M+H)⁺.

1
2
3 Step 2: A round-bottom flask was charged with 4-iodo-1-methyl-1*H*-pyrazole-5-carboxamide (222
4 g, 886 mmol) and DCM (2.22 L) and the reaction mixture was cooled to 0 °C. 2,6-Lutidine (310
5 mL, 2.66 mol) and TFAA (253 mL, 1.77 mol) were added. After reaction was complete, saturated aq
6 NaHCO₃ (800 mL) was added and the layers separated. The aqueous layer was washed with DCM
7 (800 mL). The organic layers were combined and washed with saturated aq NH₄Cl (800 mL), 1*N*
8 HCl (800 mL), and brine (800 mL). The organic layer was dried over MgSO₄, filtered, and
9 concentrated in vacuo. The residue was suspended in heptanes (~2 L) and granulated at 0–5 °C for
10 30 min. The solid was collected via filtration and dried in a vacuum oven to afford 4-iodo-1-methyl-
11 1*H*-pyrazole-5-carbonitrile as a colorless solid (196 g, 95% yield). Steps 1 and 2 were repeated with
12 minor modifications to provide 7.2 kg of **8**. ¹H NMR (CDCl₃) δ 7.60 (s, 1H), 4.09 (s, 3H). ¹³C NMR
13 (151 MHz, CDCl₃) δ:144.8, 120.9, 110.0, 66.7, 39.4. UPLC (UPLC-MS Method 1): t_R = 0.70 min.
14 MS (ES⁺): 233.8 (M+H)⁺.
15
16
17
18
19
20
21
22
23
24
25
26
27
28
29
30
31

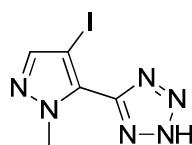
32 *tert*-butyl (3*R*)-3-{{[4-(5-cyano-1-methyl-1*H*-pyrazol-4-yl)benzoyl](3-methylpyridin-2-
33 yl)amino}piperidine-1-carboxylate (**9**)
34
35
36



51 4-Bromobenzamide **6** (2.67 g, 5.12 mmol), nitrile **8** (1.19 g, 5.12 mmol), Pd₂(dba)₃ (234 mg, 0.256
52 mmol), and XPhos (257 mg, 0.512 mmol) were dissolved in dioxane (27 mL) under nitrogen
53
54
55

1
2
3 atmosphere. A solution of Na₂CO₃ (1.63 g, 15.4 mmol) in water (3 mL) was added. The mixture
4
5 was heated at 80 °C for 6 h, then stirred at rt overnight. The reaction mixture was diluted with
6
7 EtOAc (150 mL) and washed with 50% brine solution (100 mL). The separated organic phase was
8
9 dried over MgSO₄, filtered and concentrated. The residue was purified by silica gel column
10
11 chromatography eluting with a gradient of 15–100% EtOAc/heptane to afford *tert*-butyl (3*R*)-3- $\{[4-$
12
13 (5-cyano-1-methyl-1*H*-pyrazol-4-yl)benzoyl](3-methylpyridin-2-yl)amino $\}$ piperidine-1-carboxylate
14
15 as a colorless solid (1.87 g, 73% yield). ¹H NMR (CDCl₃) δ : 8.43 (m, 1H), 7.72 (s, 1H), 7.40–7.35
16
17 (m, 5H), 7.21–7.02 (m, 1H), 4.87–4.32 (m, 2H), 4.07 (s, 3H), 3.49 (d, 1H), 2.82–2.21 (m, 2H), 2.05
18
19 (s, 3H), 1.80–1.48 (m, 4H), 1.47 (d, 9H). ¹³C NMR (CDCl₃) δ : 169.1, 154.8, 153.2, 146.8, 140.0,
20
21 137.1, 136.7, 131.8, 130.7, 129.3, 128.7, 125.5, 123.3, 112.1, 111.1, 79.6, 55.0, 48.2, 43.7, 38.5,
22
23 28.4, 28.2, 27.5, 25.1, 17.8. UPLC (UPLC-MS Method 1): t_R = 1.01 min. MS (ES⁺): 501.4 (M+H)⁺.
24
25 HRMS (m/z) [M+H]⁺ calcd for C₂₈H₃₃N₆O₃, 502.2638; found, 502.265.
26
27
28
29
30
31
32

33
34 5-(4-iodo-1-methyl-1*H*-pyrazol-5-yl)-2*H*-tetrazole (**10**)
35



42 Caution: This reaction generates hydrazoic acid and requires appropriate safety measures. Sodium
43
44 azide is highly toxic.
45

46 Original Method:
47

48 The nitrile **8** (462 mg, 1.98 mmol, 1 eq) was dissolved in DMF (2 mL). To this solution was added
49
50 NaN₃ (387 mg, 4.66 mmol, 2.4 eq) and NH₄Cl (318 mg, 5.95 mmol, 3 eq). A blast shield was
51
52 placed in front of the reaction set up, then the reaction mixture was heated to 120 °C. After 3 h,
53
54

1
2
3 LCMS indicated reaction was complete. The mixture was diluted with water, cooled to 0 °C and
4
5 quenched using 20% aq NaNO₂ followed by addition of 20% aq H₂SO₄ until the pH of the mixture
6
7 was 3. A solid precipitated and was collected via suction filtration using a Buchner funnel with a
8
9 paper filter to afford 478 mg (88%) of tetrazole **10**.

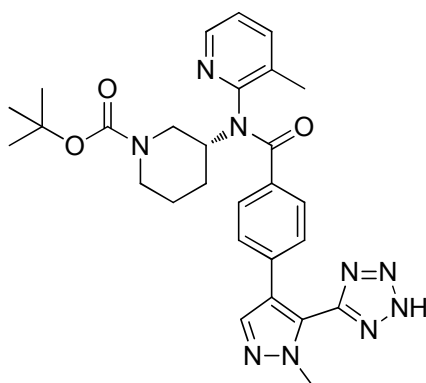
11
12 Generation 1:

13
14 A 50 L reactor was charged with DMF (16.9 kg) and water (5.8 kg) followed by nitrile **8** (4.5 kg,
15
16 19.3 mol). To the slurry was added NH₄Cl (2.1 kg, 38.6 mol) and NaN₃ (2.5 kg, 38.6 mol). The inlet
17
18 and outlet were positioned at opposite sides of the glass lid and the reactor content was swept with
19
20 nitrogen to a 25% NaOH scrubber. The flow rate was not measured, but remained strong enough to
21
22 ensure bubbling through the scrubber to mitigate the risk of exposure to hydrazoic acid during the
23
24 course of the reaction. The slurry was then heated to 90 °C for 16 h after which time HPLC assay
25
26 showed 99.6% conversion. The mixture was cooled to 5 °C and water (11.6 kg) was added and
27
28 proper reactor venting was ensured. The reaction was quenched by the addition of a 40 wt% NaNO₂
29
30 solution (3.4 kg, 19.3 mol of NaNO₂). Next, a 32% HCl solution (7.2 kg) was added to the reactor to
31
32 a final pH of 0.5, inducing precipitation of tetrazole **10** in the process. (**Note:** aq HCl was preferred
33
34 over sulfuric acid for large scale work since it provided a mixture without precipitate because of the
35
36 formation of NaCl instead of the less soluble Na₂SO₄). A Nutsche filter was pressurized with
37
38 nitrogen, then the mixture was filtered and the solids were washed with water (10.1 kg). The solids
39
40 were dried initially by flowing air through the Nutsche filter followed by air drying on trays to
41
42 afford tetrazole **10** (4.8 kg, 99.8 area% by HPLC, 89.1% yield). ¹H NMR (MeOH-d₄) δ 7.69 (s, 1H),
43
44 4.08 (s, 3H). ¹³C NMR (MeOH-d₄) δ 151.8, 146.2, 132.8, 62.2, 39.9. UPLC (UPLC-MS Method 1):
45
46 t_R = 0.52 min. MS (ES⁺): 276.9 (M+H)⁺.

Generation 2:

A 500 mL reactor was charged with IPA (100 mL) and water (100 mL) followed by nitrile **8** (20 g, 86 mmol). To the slurry was added ZnBr₂ (1.9 g, 8.6 mmol). The reactor content was swept with nitrogen to a 20% NaOH scrubber to mitigate the risk of exposure to hydrazoic acid during the course of the reaction. The slurry was then heated to 75 °C. To the homogeneous solution was added NaN₃ (11.2 g, 172 mmol). After 47 h HPLC assay showed 95.7% conversion. The mixture was cooled to 5 °C. The reaction was quenched by the addition of a 20 wt% NaNO₂ solution (44.42 g, 129 mmol of NaNO₂). Next, a 20% HCl solution (58.4 g) was added to the reactor to a final pH of ca. 1, inducing precipitation of tetrazole **10** in the process. The mixture was filtered on a Buchner filter, the solids were washed with cold water, and dried in air to afford tetrazole **10** (20.06 g, 98 area% by HPLC, 84.6% yield).

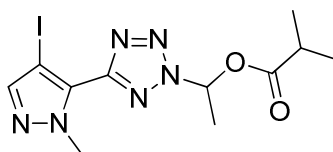
tert-butyl (3*R*)-3-(4-(1-methyl-5-(2*H*-tetrazol-5-yl)-1*H*-pyrazol-4-yl)-*N*-(3-methylpyridin-2-yl)benzamido)piperidine-1-carboxylate (**11**)



A round-bottom flask was charged with *tert*-butyl (3*R*)-3-{{(3-methylpyridin-2-yl)[4-(4,4,5,5-tetramethyl-1,3,2-dioxaborolan-2-yl)benzoyl]amino}piperidine-1-carboxylate **6** (1.53 g, 2.93 mmol)

1
2 and 5-(4-iodo-1-methyl-1*H*-pyrazol-5-yl)-2*H*-tetrazole **10** (674 mg, 2.44 mmol). To this was added
3
4 dioxane (12.2 mL) and aq NaOH (4.07 mL, 3M solution, 12.2 mmol). The reaction mixture was
5
6 heated to 70 °C under nitrogen atmosphere for 30 min. To a vial was added the Pd(OAc)₂ (34.3 mg,
7
8 0.153 mmol) and cataCXium[®] A (123 mg, 0.342 mmol). The atmosphere was exchanged for
9
10 nitrogen, and toluene was added. The catalyst was stirred at rt for 15 min, until a bright yellow
11
12 slurry formed. At this point, the catalyst was added to the reaction mixture, and the temperature was
13
14 adjusted to 100 °C. The reaction mixture was stirred for 3 h at 100 °C. After complete consumption
15
16 of the starting material, the reaction was concentrated under reduced pressure, then water (10 mL)
17
18 was added. The reaction mixture was extracted with MTBE (3x 25 mL). The aq phase was cooled to
19
20 0 °C, and 1M HCl was added dropwise to form a precipitate which was collected *via* suction
21
22 filtration and dried in vacuo to obtain *tert*-butyl (3*R*)-3-(4-(1-methyl-5-(2*H*-tetrazol-5-yl)-1*H*-
23
24 pyrazol-4-yl)-*N*-(3-methylpyridin-2-yl)benzamido)piperidine-1-carboxylate **13** (1.2 g, 90%). ¹H
25
26 NMR (MeOH-d₄) δ: 8.42 (d, 1H), 7.80 (s, 1H), 7.72–7.51 (m, 1H), 7.30–7.05 (m, 5H), 4.62–4.44
27
28 (m, 2H), 4.18–3.98 (m, 2H), 3.95 (s, 3H), 2.75–2.62 (m, 1H), 2.18–2.04 (m, 2H), 1.79–1.70 (m, 2H),
29
30 1.53–1.42 (m, 4H), 1.31 (s, 9H). ¹³C NMR (101 MHz, CDCl₃, 55 °C) δ: 172.2, 156.6, 154.0, 152.4,
31
32 147.9, 142.0, 139.0, 136.2, 135.4, 133.8, 129.8, 129.0, 127.9, 125.3, 124.7, 81.4, 56.5, 45.2, 38.4,
33
34 33.1, 28.8, 26.2, 18.1. UPLC (UPLC-MS Method 1): t_R = 0.82 min. MS (ES⁺): 544.4 (M+H)⁺.
35
36 HRMS (*m/z*) [M+H]⁺ calcd for C₂₈H₃₄N₉O₃, 544.2779; found, 544.2771.
37
38
39
40
41
42
43
44
45
46

47 1-[5-(4-iodo-1-methyl-1*H*-pyrazol-5-yl)-2*H*-tetrazol-2-yl]ethyl 2-methylpropanoate (*rac*-**12**)
48
49
50
51
52
53
54
55
56
57
58
59
60



A round-bottom flask with a stir bar was charged with tetrazole **10** (8.00 g, 29.0 mmol, 1.00 equiv.), THF (100 mL), DMAP (212 mg, 1.74 mmol, 0.060 equiv.), acetaldehyde (1.95 mL, 34.8 mmol, 1.20 equiv.) and Et₃N (4.85 mL, 34.8 mmol, 1.20 equiv) followed by isobutyric anhydride (5.29 mL, 31.9 mmol, 1.10 equiv). The reaction mixture was stirred at rt for 16 h. The reaction mixture was poured into water (100 mL), transferred to a separatory funnel, and extracted with 2 volumes of EtOAc (2 x 100 mL). The combined organic layers were washed with brine, dried and concentrated in vacuo. The crude product was purified by silica gel chromatography, eluting with a 0–40% gradient of EtOAc in heptane to yield 5.58 g of *rac*-**12** (49% yield). *R_f* = 0.29 (heptane/EtOAc 4:1 (v/v)). NMR Spectroscopy: ¹H NMR (400 MHz, CDCl₃, 25 °C, δ): 7.62 (s, 1H), 7.38 (q, *J*=6.2 Hz, 1H), 4.22 (s, 3H), 2.62 (qq, *J*=7.0, 7.0 Hz, 1H), 2.04 (d, *J*=6.2 Hz, 3H), 1.20 (d, *J*= 6.8 Hz, 3H), 1.17 (d, *J*= 6.8 Hz, 3H). ¹³C NMR (101 MHz, CDCl₃, 25 °C, δ): 174.9, 156.7, 145.3, 131.6, 80.4, 60.8, 40.4, 33.8, 19.5, 18.8, 18.7. IR (thin film, cm⁻¹): 1754, 1328, 1184, 1085, 992, 957, 845, 755. HRMS (*m/z*): calculated for C₁₁H₁₆IN₆O₂ [M + H]⁺ 391.0374; found 391.0370.

(S)-1-(5-(4-Iodo-1-methyl-1*H*-pyrazol-5-yl)-2*H*-tetrazol-2-yl)ethyl isobutyrate (*(S)*-**12**)

A reactor purged with nitrogen was charged with MTBE (125 L), 5-(4-iodo-1-methyl-1*H*-pyrazol-5-yl)-2*H*-tetrazole (**10**), (2.50 kg, 9.06 mol, 1.00 equiv), ((*2S*)-2-(bis(3,5-bis(trifluoromethyl)phenyl)hydroxymethyl)-1-pyrrolidinyl)(4-(1-pyrrolidinyl)-3-pyridinyl)methanone **14** (188 g, 0.269 mol, 3 mol%). The reactor was cooled to 2 °C. While

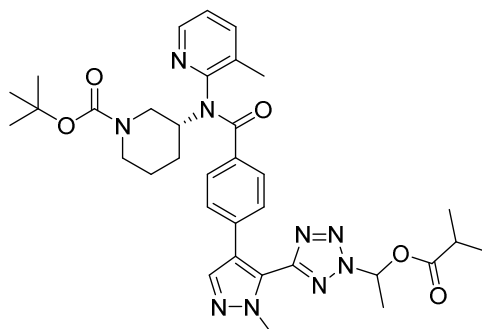
1
2
3 maintaining an internal temperature of -5–5 °C, acetaldehyde (0.808 kg, 18.3 mol, 2.02 equiv) was
4
5 added followed by Et₃N (1.37 kg, 13.5 mol, 1.49 equiv), and lastly isobutyric acid (2.15 kg, 13.6
6
7 mol, 1.50 equiv). The internal temperature was held between -5–5 °C for 14 h, at which point a
8
9 sample indicated >99% conversion to product. The reaction mixture was concentrated in vacuo to
10
11 approximately 38 L. The temperature was adjusted to 16 °C. With the internal temperature
12
13 maintained at 15–30 °C, water (25 L) was added, and the reaction mixture was agitated for 30 min.
14
15 The layers were allowed to separate and the aqueous layer removed. The organic layer was
16
17 concentrated in vacuo to approximately 15 L. Three times MeOH (50 L) was added to the reaction
18
19 mixture and then concentrated in vacuo to approximately 15 L. The process was repeated on the
20
21 same scale to afford enantio-enriched (S)-**12** as a solution in MeOH for further processing.
22
23 Enantiomeric ratio (er) determination (Lux Amylose-2 column; eluent B: MeOH/MeCN 1:1): 97:3.
24
25 The minor isomer was removed by chromatography on chiral support under the following
26
27 conditions:
28
29
30
31

32	Column	Chiralpak IC, 30x25 cm, 20μ
33	Column Temp.	Ambient
34	Mobile Phase	100% MeOH
35	Feed Concentration	125 g/L in MeOH
36	Injection Volume	500 mL
37	Flow Rate	2 L/min
38	Wavelength	300 nm
39	Injection Interval	20 min
40		
41		
42		
43		
44		
45		
46		
47		
48		
49		
50		
51		
52		
53		
54		
55		
56		
57		
58		
59		
60		

1
2
3 After separation, the collected fractions were concentrated to remove most of the MeOH. Five 15 kg
4
5 back additions of THF were made to the thick oil to remove any remaining MeOH. Assay showed
6
7 residual MeOH at 0.06% and 99.93% chiral purity/98.28% achiral purity. ^1H NMR (CDCl_3) δ : 7.62
8
9 (s, 1H), 7.38 (q, $J=6.2$ Hz, 1H), 4.22 (s, 3H), 2.62 (qq, $J=7.0, 7.0$ Hz, 1H), 2.04 (d, $J=6.2$ Hz, 3H),
10
11 1.20 (d, $J= 6.8$ Hz, 3H), 1.17 (d, $J= 6.8$ Hz, 3H). ^{13}C NMR (CDCl_3) δ : 174.9, 156.7, 145.3, 131.6,
12
13 80.4, 60.8, 40.4, 33.8, 19.5, 18.8, 18.7. IR (thin film, cm^{-1}): 1754, 1328, 1184, 1085, 992, 957, 845,
14
15 755. HRMS (m/z): calculated for $\text{C}_{11}\text{H}_{16}\text{N}_6\text{O}_2$ [$\text{M} + \text{H}$] $^+$ 391.0374; found 391.0370.
16
17
18
19
20
21

22 (*R*)-3-[(4-{5-[2-((*S*)-1-Isobutyryloxy-ethyl)-2*H*-tetrazol-5-yl]-1-methyl-1*H*-pyrazol-4-yl}-benzoyl)-
23
24 (3-methyl-pyridin-2-yl)-amino]-piperidine-1-carboxylic acid tert-butyl ester ((*R,S*)-**13**)
25

26 (*R*)-3-[(4-{5-[2-((*S*)-1-Isobutyryloxy-ethyl)-2*H*-tetrazol-5-yl]-1-methyl-1*H*-pyrazol-4-yl}-benzoyl)-
27
28 (3-methyl-pyridin-2-yl)-amino]-piperidine-1-carboxylic acid tert-butyl ester ((*R,R*)-**13**)
29
30
31



43 A 3-necked round-bottom flask fitted with a reflux condenser, rubber septa, and stir bar was charged
44
45 with CsF (6.42 g, 42.3 mmol, 3.00 equiv), water (40 mL), and dioxane (40 mL). A nitrogen/vacuum
46
47 line was used to evacuate and backfill the setup with nitrogen 3 times. Under a nitrogen
48
49 atmosphere, the reaction mixture was heated at 70 °C for 30 min. In a separate round-bottom flask,
50
51 compound **12** (5.50 g, 14.1 mmol, 1.00 equiv) was dissolved in dioxane. Nitrogen gas was bubbled
52
53
54

1
2 through the solution for 20 min. To the original flask under positive nitrogen pressure was added
3 boronic ester **6** (9.82 g, 16.9 mmol, 1.20 equiv), PdCl₂(amphos) (499 mg, 0.705 mmol, 0.050 equiv)
4 followed by the dioxane solution of **12**. The cloudy yellow reaction mixture was stirred and heated
5 at 75 °C for 90 min. The reaction mixture was cooled and poured into saturated aq NH₄Cl (100 mL),
6 transferred to a separatory funnel, and extracted from with 2 volumes of EtOAc (2 x 250 mL). The
7 combined organic layers were washed with brine, dried and concentrated in vacuo. The crude
8 product was purified by silica gel chromatography, eluting with a 10–100% gradient of EtOAc in
9 heptane to yield 6.76 g of a diastereomeric mixture of the product (73% yield). The diastereomeric
10 mixture was separated via Chiral Preparative Chromatography Method 2. The first peak to elute was
11 (*R,R*)-**13** and the second peak to elute was (*R,S*)-**13**, which afforded 3.10 g (3.38 g theoretical max,
12 92% yield), 96% d.r. of the latter compound.
13
14
15
16
17
18
19
20
21
22
23
24
25
26
27
28
29
30

31 Analytical data for (*R,R*)-**13**: ¹H NMR (CDCl₃) δ: 8.40 (br s, 1H), 7.60 (s, 1H), 7.35 (br s, 1H), 7.30
32 (q, 1H), 7.23 (br s, 2H), 7.17–7.08 (br m, 3H), 4.48 (br d, 1H), 4.16–3.95 (br m, 4H), 3.42 (br s, 1H),
33 2.63–2.50 (m, 2H), 2.39 (br s, 1H), 2.05–1.98 (br m, 3H), 1.94 (d, 3H), 1.67–1.57 (br m, 4H), 1.49–
34 1.43 (br d, 9H), 1.19 (d, 3H), 1.14 (d, 3H). ¹³C NMR (CDCl₃, 50 °C) δ: 174.6, 169.6, 157.1, 154.8,
35 153.6, 146.7, 140.0, 138.5, 135.4, 133.6, 131.9, 128.6, 127.6, 126.9, 124.3, 123.2, 100.0, 80.3, 64.3,
36 54.8, 44.1, 39.0, 33.7, 28.5, 25.2, 19.4, 18.6, 18.5, 17.9, 13.6. UPLC (UPLC-MS Method 1): t_R =
37 1.07 min. MS (ES⁺): 658.4 (M+H)⁺.
38
39
40
41
42
43
44
45
46

47 Analytical data for (*R,S*)-**13**: ¹H NMR (CDCl₃) δ: 8.40 (br s, 1H), 7.60 (s, 1H), 7.34 (br s, 1H), 7.30
48 (q, 1H), 7.23 (br s, 2H), 7.17–7.07 (br m, 3H), 4.48 (br d, 1H), 4.15–3.95 (br m, 4H), 3.42 (br s, 1H),
49 2.63–2.50 (m, 2H), 2.39 (br s, 1H), 2.05–1.93 (br m, 6H), 1.76–1.62 (br m, 4H), 1.50–1.42 (br m,
50
51
52
53
54
55
56
57
58
59
60

1
2
3 9H), 1.19 (d, 3H), 1.14 (d, 3H). ^{13}C NMR (CDCl_3 , 50 °C) δ : 174.6, 169.6, 157.1, 154.8, 153.6,
4
5 146.7, 140.0, 138.5, 135.4, 133.6, 131.9, 128.6, 127.6, 126.9, 124.3, 123.2, 100.0, 80.3, 64.3, 54.8,
6
7 44.1, 39.0, 33.7, 28.5, 25.2, 19.4, 18.6, 18.5, 17.9, 13.6. UPLC (UPLC-MS Method 1): t_{R} = 1.06
8
9 min. MS (ES⁺): 658.3 (M+H)⁺.

11
12
13
14 Alternative Method for the Preparation of (*R,S*)-Compound **13**:

15
16 To a solution of tetrazole **11** (7.50 g, 13.8 mmol) and catalyst **14** (965 mg, 1.38 mmol) in toluene
17
18 (69 mL) was added Et₃N (3.85 mL, 27.6 mmol), acetaldehyde (1.54 mL, 27.6 mmol), and isobutyric
19
20 anhydride (4.58 mL, 27.6 mmol). The reaction mixture was stirred at rt for 16 h. The reaction
21
22 mixture concentrated in vacuo and the residue was purified by column chromatography on silica gel,
23
24 eluting with a gradient of 20–100% EtOAc in heptane to afford the title compound as a colorless
25
26 solid (6.3 g, 69%, 70% e.e.). The solid was processed according to Chiral Preparative
27
28 Chromatography Method 2, followed by concentration to dryness in vacuo to give compound **13**
29
30 (4.65 g, 99% e.e.).
31
32
33
34
35
36
37

38 The individual diastereomers were deprotected as described in step 2 below:

39
40 (*R*)-1-(5-(1-methyl-4-(4-((3-methylpyridin-2-yl)((*R*)-1 λ 2-piperidin-3-yl)carbamoyl)phenyl)-1*H*-
41
42 pyrazol-5-yl)-2*H*-tetrazol-2-yl)ethyl isobutyrate dihydrochloride ((*R,R*)-**3**) (absolute stereochemistry
43
44 determined by X-ray crystal structure, see SI, CCDC 1571688)

45
46
47 ^1H NMR (CD_3CN) δ : 9.58 (br s, 1H), 9.17 (br s, 1H), 8.44 (d, 1H), 7.78 (br s, 1H), 7.68 (s, 1H), 7.46
48
49 (br s, 1H), 7.36–7.29 (m, 3H), 7.22–7.18 (br m, 2H), 5.05 (br s, 1H), 3.99 (s, 3H), 3.80 (br s, 1H),
50
51 3.65 (br s, 1H), 3.32 (br d, 1H), 2.92–2.77 (br m, 1H), 2.67–2.57 (m, 1H), 2.18 (br s, 4H), 2.05–2.00
52
53
54

(br m, 1H), 1.92 (d, 3H), 1.87 (br s, 1H), 1.54 (br s, 1H), 1.17 (d, 3H), 1.11 (d, 3H). ^{13}C NMR (CD_3CN , 50°C) δ : 175.4, 170.4, 157.4, 148.8, 148.0, 142.4, 138.7, 137.5, 135.6, 134.2, 128.8, 128.5, 127.6, 126.8, 123.8, 81.1, 46.1, 44.0, 39.2, 34.2, 34.0, 26.6, 22.7, 19.0, 18.6, 18.5. UPLC (UPLC-MS Method 2): $t_{\text{R}} = 1.19$ min. MS (ES $^+$): 558.4 (M+H) $^+$. HRMS (m/z) [M+H] $^+$ calcd for $\text{C}_{28}\text{H}_{36}\text{N}_9\text{O}_3$, 558.2936; found, 558.294

(*S*)-1-(5-(1-methyl-4-(4-((3-methylpyridin-2-yl)((*R*)-1 λ 2-piperidin-3-yl)carbamoyl)phenyl)-1*H*-pyrazol-5-yl)-2*H*-tetrazol-2-yl)ethyl isobutyrate dihydrochloride ((*R,S*)-**3**)

^1H NMR (CD_3CN) δ : 9.75 (br s, 1H), 9.31 (br s, 1H), 8.47 (s, 1H), 7.98 (br s, 1H), 7.68 (s, 1H), 7.60 (br s, 1H), 7.38–7.32 (m, 3H), 7.24–7.20 (br m, 2H), 5.05 (br s, 1H), 3.99 (s, 3H), 3.87 (br s, 1H), 3.68 (br s, 1H), 3.33 (br s, 1H), 2.88 (br s, 1H), 2.64–2.59 (m, 1H), 2.26 (br s, 4H), 2.07–2.01 (m, 1H), 1.94–1.86 (m, 4H), 1.60 (br s, 1H), 1.17 (d, 3H), 1.10 (d, 3H). ^{13}C NMR (CD_3CN , 50°C) δ : 175.4, 170.4, 157.4, 148.8, 148.0, 142.4, 138.7, 137.5, 135.6, 134.2, 128.8, 128.5, 127.6, 126.8, 123.8, 81.1, 46.1, 44.0, 39.2, 34.2, 34.0, 26.6, 22.2, 19.0, 18.6, 18.5. UPLC (UPLC-MS Method 2): $t_{\text{R}} = 1.19$ min. MS (ES $^+$): 558.4 (M+H) $^+$.

Largest Scale Preparation of (*R,S*)-**3**:

Step 1: In a 5 L flask, (*S*)-**12** (192.1 g, 487.4 mmol) was dissolved in THF (2000 mL) and cooled to -49.0°C . *i*PrMgCl (2.0 M) in THF (305 mL, 610 mmol, 1.3 equiv) was added over 30 min keeping the internal temperature $< -41.1^\circ\text{C}$, to give a dark orange solution. After 10 min, ZnCl_2 (1.9 M) in 2-MeTHF (175 mL, 0.68 equiv, 330 mmol) was added over 10 min. The mixture was warmed to 25°C over 50 min to give a clear yellow solution. Compound **5** (230.1 g, 485.0 mmol,

1
2
3 1.0 equiv) was added in one portion as a solid, followed by addition of
4
5 dichloro[bis(diphenylphosphinophenyl)ether]palladium(II) (2.44 g, 3.24 mmol, 0.0066 equiv) in
6
7 one portion as a solid creating an exotherm (31–47 °C over 1 min). The reaction temperature was
8
9 maintained at 45–50 °C for 25 min. After 10 min, assay showed 96.5% conversion based on **5**.
10
11 The reaction was cooled to 15 °C and quenched by adding 1 L of half-saturated NH₄Cl over 1
12
13 min. After 10 min, the organic phase was filtered through diatomaceous earth and concentrated
14
15 to give a dark brown foam, which was dissolved in 1 L of DCM and filtered through a pad of
16
17 diatomaceous earth to removed insoluble ash. The crude product was purified on a 5 kg silica gel
18
19 column eluting with 4 CV of 50% EtOAc:50% heptane (40 L) followed by 4 CV of 60%
20
21 EtOAc:40% heptane (40 L) followed by 2 CV of 70% EtOAc:30% heptane (20 L). Compound
22
23 **13** was isolated as a light orange foam (250.3 g, 78.1%) with analytical UPLC purity >99% and
24
25 chiral SFC as a single diastereomer.
26
27
28
29
30

31
32 Step 2: To a 5 L three-neck flask was charged **13** (275.5 g, 428.0 mmol) dissolved in MeCN (10
33
34 mL/g, 2.76 L). After degassing the solution, HCl (2 M) in diethyl ether (1.50 L, 3.00 mol, 7
35
36 equiv) was added over 20 min to give an amber solution. After 1.5 h, assay showed complete
37
38 deprotection. The solution was concentrated to 1.1 L and then diluted with MTBE (10 mL/g,
39
40 2.76 L). The mixture was granulated for 1 h at rt then filtered and washed with MTBE under N₂.
41
42 The cake was washed with additional MTBE. The solids were dried in a vacuum oven at 40 °C
43
44 for 72 h to provide (R,S)-**3** (241.3 g, 89.4%) as a partially crystalline dihydrochloride with
45
46 analytical UPLC purity 99.4%.
47
48
49
50
51
52

53 **Acknowledgments.** Neal Sach and Louise Bernier for high-throughput reaction screening for the
54
55 Buchwald reaction with substrate **4**. Brian Samas for obtaining the X-ray crystal structure of
56
57
58
59
60

(*R,R*)-**13**. Li-Jen Ping and Mark Bundesmann for chemistry support and PCSK9 project team members Kim McClure, Etzer Darout and Bob Dullea for their input.

Associated Content

Supporting Information

Alternative preparation of compound **10**, X-ray crystal structure of (*R,R*)-**3**, data for the torsion angle scan of (*S*)-**12** and NMR spectra. This material is available free of charge via the Internet at <http://pubs.acs.org>.

Author Information

Corresponding Authors

*E-mail: david.w.piotrowski@pfizer.com, jerry.salan@nalasengineering.com

Notes

The authors declare the following competing financial interest(s): This work was funded by Pfizer. All Pfizer authors were employed by Pfizer Inc at the time this work was done. Compound **2** (PF-06446846) is commercially available via MilliporeSigma (catalog # PZ0374).

References

¹ (a) Robinson, J. G.; Farnier, M.; Krempf, M.; Bergeron, J.; Luc, G.; Aversa, M.; Stroes, E. S.; Langslet, G.; Raal, F. J.; El Shahawy, M.; Koren, M. J.; Lepor, N. E.; Lorenzato, C.; Pordy, R.; Chaudhari, U.; Kastelein, J. J. P. *N. Engl. J. Med.* **2015**, *372*, 1489–1499. (b) Sabatine, M. S.; Giugliano, R. P.; Wiviott, S. D.; Raal, F. J.; Blom, D. J.; Robinson, J.; Ballantyne, C. M.; Somaratne, R.; Legg, J.; Wasserman, S. M.; Scott, R.; Koren, M. J.; Stein, E. A. *N. Engl. J. Med.*, **2015**, *372*, 1500–1509.

² (a) Petersen, D. N.; Hawkins, J.; Ruangsiriluk, W.; Hepworth, D.; Loria, P. M.; Carpino, P. A. *Cell Chem. Biol.* **2016**, *23*, 1362–1371. (b) Lintner, N.; McClure, K.; Petersen, D.; Londregan, A.; Piotrowski, D.; Wei, L.; Xiao, J.; Bolt, M.; Loria, P.; Maguire, B.; Geoghegan, K.; Huang, A.; Rolph, T.; Liras, S.; Doudna, J.; Dullea, R.; Cate, J. A. *PLOS Biology* **2017**, *15*, e2001882/1-e2001882/36.

³ Hydrazoic acid reacts directly with nitriles to provide tetrazoles, see: Mihina, J. S.; Herbst, R. *M. J. Org. Chem.*, **1950**, *15*, 1082–1092. The use of a continuous flow reactor can provide safe

1
2
3
4
5 alternative for the direct generation and use of hydrazoic acid, see: Gutmann, B.; Obermayer, D.;
6 Roduit, J.-P.; Roberge, D. M.; Kappe, C. O. *J. Flow Chem.* **2012**, *2*, 8-19.

7
8
9 ⁴ (a) Dufert, M. A.; Billingsley, K. L.; Buchwald, S. L. *J. Am. Chem. Soc.* **2013**, *135*, 12877–
10 12885. (b) Cousaert, N.; Toto, P.; Willand, N.; Deprez, B. *Tetrahedron Lett.* **2005**, *46*, 6529–
11 6532.

12
13 ⁵ (a) Piotrowski, D. W.; Kamlet, A. S.; Dechert-Schmitt, A.-M. R.; Yan, J.; Brandt, T. A.; Xiao,
14 J.; Wei, L.; Barrila, M. T. *J. Am. Chem. Soc.* **2016**, *138*, 4818–4823. (b) Kinens, A.; Sejejs, M.;
15 Kamlet, A. S.; Piotrowski, D. W.; Vedejs, E.; Suna, E. *J. Org. Chem.* **2017**, *82*, 869–886.

16
17 ⁶ X-ray structure for (*R,R*)-**3** and associated data can be found in the supporting information. The
18 Cambridge Crystallographic Data Centre accession number is CCDC 1571688.

19
20 ⁷ (a) Wiss, J.; Fleury, C.; Onken, U. *Org. Process Res. Dev.* **2006**, *10*, 349–353. (b) Bräse, S.;
21 Gil, C.; Knepper, K.; Zimmermann, V. *Angew. Chem. Int. Ed.* **2005**, *44*, 5188–5240.

22
23 ⁸ Yakovleva, G. S.; Kurbangalina, R. K.; Stesik, L. N. *Combust. Explos. Shock Waves* **1977**, *13*,
24 405–407.

25
26 ⁹ (a) Wiss, J.; Fleury, C.; Heugerber, C.; Onken, U.; Glor, M. *Org. Process Res. Dev.* **2007**, *11*,
27 1096–1103. (b) Shapiro, E. L. *Chem. Eng. News* **1974**, *52*, 5.

28
29 ¹⁰ (a) *Recommendations on the Transport of Dangerous Goods, Test 3(a)(i) Third Edition,*
30 *United Nations, New York and Geneva, 1999.* (b) *TB 700-2, Department of Defense Explosives*
31 *Hazard Classification Procedures, 5-4 (a), January 1998.*

32
33 ¹¹ See, Treitler, D. S.; Leung, S.; Lindrud, M. *Org. Process Res. Dev.* **2017**, *21*, 460–467 for a
34 summary of tetrazole synthetic methods employing azide and a wide range of catalysts.

35
36 ¹² (a) Demko, Z. P.; Sharpless, K. B. *J. Org. Chem.* **2001**, *66*, 7945–7950. (b) Himo, F.; Demko,
37 Z. P.; Noodleman, L.; Sharpless, K. B. *J. Am. Chem. Soc.*, **2003**, *125*, 9983–9987. (c) Girardin,
38 M.; Dolman, S. J.; Lauzon, S.; Ouellet, S. G.; Hughes, G.; Fernandez, P.; Zhou, G.; O'Shea, P.
39 *Org. Process Res. Dev.* **2011**, *15*, 1073–1080. (d) Girardin, M.; Dolman, S. J.; Lauzon, S.;
40 Ouellet, S. G.; Hughes, G.; Fernandez, P.; Zhou, G.; O'Shea, P. D. *Org. Process Res. Dev.* **2011**,
41 *15*, 1073–1080.

42
43 ¹³ Patnaik, P. *Handbook of Inorganic Chemicals*; McGraw-Hill: New York, 2002; p 341.

44
45 ¹⁴ Hansen, M. M.; Jolly, R. A.; Linder, R. J. *Org. Process Res. Dev.* **2015**, *19*, 1507–1516.
46
47
48
49
50
51
52
53
54
55
56
57
58
59
60